Use of Magnetic Resonance Imaging To Study Transport of Methanol in Poly(methyl methacrylate) at Variable Temperature

Monique Ercken, Peter Adriaensens, Guy Reggers, Robert Carleer, Dirk Vanderzande, and Jan Gelan*

Departement SBG, Instituut voor Materiaalonderzoek (IMO), Limburg University, Universitaire Campus, Gebouw D, B-3590 Diepenbeek, Belgium

Received January 30, 1996; Revised Manuscript Received May 9, 1996[⊗]

ABSTRACT: The transport kinetics of methanol in PMMA have been studied over the temperature range 25−60 °C, using magnetic resonance imaging. It is shown that transport behavior changes from being relaxation controlled (Case II) at the lowest temperature to approaching Fickian behavior at the higher temperatures. It is also shown that the change of the exponent of time, *n*, describing the methanol uptake, with the swelling temperature can be compared with a change of the mechanical behavior of the polymer matrix in the presence of the penetrant. From DSC and DMA measurements, it can be concluded that the transition from Case II toward Fickian diffusion takes place at a temperature around the effective T_g of the imbibed material.

Introduction

The transport of liquids in polymers is of importance in both the manufacture and end application of polymers. Much interest surrounds the motion of monomer, solvent, or plasticizer molecules in polymers.[1−4] It becomes increasingly important in the field of controlled drug release[5] and applications such as microlithography, membrane separation, and ultrafiltration.[6−8]

Polymer−solvent systems exhibit a wide range of diffusion phenomena, going from common Fickian diffusion to Case II diffusion.[9−12] These diffusion characteristics represent the limited responses of polymers to the solvent and have substantially different characteristics. Fickian (or Case I) diffusion is characterized by an increase in solvent concentration going from the inside of the polymer to the fully swollen regions at the outside of the sample, for which the rate of diffusion is much less than that of the segmental polymer relaxation rates. This behavior is also called diffusion-controlled. The distance diffused by a species is proportional to the square root of diffusion time, and the T_2 NMR relaxation time is relatively constant throughout the swollen part. This picture commonly applies to rubbery polymers. Case II behavior, on the other hand, has the following characteristics: (1) A sharp concentration boundary between the polymer core and the swollen region of the sample is present. (2) The concentration throughout the swollen region is constant. (3) The front advances through the glass at constant velocity. (4) The T_2 relaxation time decreases toward the unaffected polymer core. Since for Case II a sharp front moves into the polymer at a rate independent of its position, it implies that the diffusion of molecules through the swollen layer up to the front is not the rate-controlling process; otherwise, the rate of front advance would necessarily decrease with increasing penetration depth. The rate-controlling process must be occurring at the front and can be regarded as the movement of polymer segments in response to an osmotic swelling stress. This behavior is also called relaxation-controlled, because the diffusion is much faster than that of polymer segmental relaxation. It commonly applies to polymers in the glassy state. It must be mentioned that the type of diffusional behavior observed for any polymer−solvent system will vary with temperature and penetrant activity. Indeed, over a sufficiently wide range of temperature and/or penetrant activity, a system should exhibit both types of behavior mentioned above.

Fickian and Case II can be viewed as the two limiting types of transport process, with "anomalous" behavior (based on the contributions of both processes) lying between them. Solving Fick's second law,[12] one can express the time dependence of the distance diffused by a species as:

$$\log(\text{distance}) \sim n \times \log(\text{time}) \qquad (1)$$

where *n* theoretically lies between 0.5 for pure Fickian diffusion and 1.0 for pure Case II diffusion.

Since magnetic resonance imaging (MRI) is rather sensitive to protons of mobile solvent molecules, it is particularly well suited for studying diffusion processes[12−20] of small molecules. One of the major advantages, as compared with weight gain measurements, is its ability to provide a visual presentation of the spatial distribution of diluent in the polymer without interrupting the diffusion process or destroying the sample. Hence, the diffusion process may be studied as long as desired on a single sample, eliminating many of the systematic errors associated with other techniques (weight gain measurements, optical microscopy, etc.).

In this paper, we shall present a detailed study of the transport of methanol in PMMA rods from ambient temperature up to near the boiling point of the penetrant and show how the transport behavior changes from being almost completely relaxation (or creep) controlled (Case II) at the lowest temperature to approaching Fickian behavior at the highest temperatures. The change of the time dependence of the diffusion distance (*n* value) as a function of temperature will be discussed in more detail.

Experimental Section

Materials. A poly(methyl methacrylate) rod (PMMA, ME307910) with a diameter of 10.5 mm was purchased from Goodfellow Cambridge Limited, England. The methanol (p.a. grade) was purchased from Janssen Chimica. The PMMA has a molecular weight $\bar{M}_w$ of 1.5×10^7 g mol^{-1} and $\bar{M}_w/\bar{M}_n \geq 6$.

[⊗] Abstract published in *Advance ACS Abstracts,* July 1, 1996.

S0024-9297(96)00155-6 CCC: $12.00 © 1996 American Chemical Society

Magnetic Resonance Imaging Experiments. Time-resolved MRI images of the diffusion process in the polymer matrix were generated at 9.4 T using a Unity 400 Varian vertical bore spectrometer equipped with a microimaging probe permitting a maximum sample size of 25 mm in diameter. Since the solvents were continuously surrounding the polymer samples, the diffusion process was never interrupted. All the images have an in-plane pixel resolution of about 70 × 70 μm in a field of view of 25 × 25 mm. Slices of 4 mm in thickness were selected in the middle of the specimen. Moreover, a Teflon stopper was placed on top of the rods to minimize longitudinal solvent diffusion. The rods, 30 mm in length, were laid along the direction of the main magnetic field (z direction) so that radial diffusion into the rods (xy plane) could be imaged. A common spin−warp sequence with a repetition time TR of 1 s and a spin−echo time TE of 13 ms was used. The ingress of methanol was followed chemical shift selectively, using a Gaussian-shaped pulse, by imaging the CH_3 signal. The surrounding solvent, having a different T_1 relaxation time than the imbibed solvent, was suppressed by using the inversion−recovery method (the inversion time TI, approximately 0.57 s, was slightly varied with temperature). This eliminates problems, due to a difference in dynamic range between the intensity of the free solvent compared to the imbibed solvent, allowing a more accurate measurement of the diffusion distance. Suppressing the surrounding solvent also permits the receiver gain to be increased to the level of the imbibed solvent rather than to the more intense bulk solvent. The ingress at the four highest temperatures was measured directly without inversion−recovery, since at these temperatures the T_1 relaxation time of the imbibed solvent becomes similar to the T_1 relaxation time of the free solvent (toward the Fickian character regime).

The front penetration will be represented in two ways: (1) by the distance s from the surface of the swollen polymer to the advancing front (directly measured on the images) and (2) by the distance d determined by the following formula:

$$\text{diffusion distance } d = \frac{\text{original sample diameter} - c}{2} \quad (2)$$

where c (measured on the images) is the diameter of the remaining glassy core. In this way, the diffusion processes alone can be evaluated by correcting for the swelling of the polymer matrix.

Differential Scanning Calorimetry. The effective glass transition temperature measurements of PMMA samples, which had absorbed methanol at specific temperatures, were conducted using a Perkin-Elmer DSC7. Each sample saturated in methanol, having a total weight of about 40 mg, was enclosed in a regular aluminum pan. This aluminum pan was sealed to keep the methanol in the PMMA. The sample was heated from −40 to 120 °C at a heating rate of 10 °C/min. The T_g of the original material is 115 °C.

Dynamic Mechanical Measurements. Rectangular sheets (dimensions 40 × 11 × 2 mm) were cut from a standard PMMA sheet (also purchased from Goodfellow, ME303020) and were swollen in methanol at different temperatures. The swollen sample was mounted between two serrated vertical clamps and was deformed under a fixed oscillating stress (1 Hz) with an oscillation amplitude of 0.6 mm, using a DuPont 983 dynamic mechanical analyzer equipped with a LNCA II cooling accessory. By knowing the sample geometry and measuring the driver signal and phase angle, the flexure storage modulus E' can be calculated. The sample was heated from 0 to 100 °C under nitrogen at a heating rate of 5 °C/min. For each swelling temperature, three samples were investigated.

Results and Discussion

As an illustration, a typical image of the time-resolved diffusion of methanol in a PMMA rod (dimensions 10.5 × 30 mm) for the lowest temperature is presented in Figure 1. Figure 2 shows three plots of the diffusion distance d (corrected for the minor swelling of the matrix) of methanol into PMMA at different temperatures. During the measurements of the time-course experiment at 26 °C, there was a short interruption between 8500 and 10 500 min. As can be seen, penetration rate increases with increasing temperature. Penetration at the lowest temperature (Figure 2a) is clearly linear with time. This behavior is typical for Case II transport.[12] The front therefore penetrates the glassy core at a constant rate, independent of its position. Under these circumstances, the rate-controlling factor must be a segmental "relaxation" process imposed on the material at the front which occurs much more slowly than does diffusion of methanol molecules up to the front. This relaxation process can be viewed in terms of the creeping of polymer segments in response to the deviatoric component of a swelling stress.[21,22] As a function of the swelling temperature, it is shown that the transport kinetics of methanol in PMMA gradually change from those typical of Case II at ambient temperatures to behavior approaching "Fickian" as the temperature is increased up to almost the boiling point of methanol (boiling point of methanol is 65 °C). As temperature increases, the velocity of the front penetration becomes dependent on its position, a deceleration being observed as it penetrates further into the specimen (see Figure 2b). Unlike Case II diffusion, Fickian diffusion moves linearly with the square root of time,[12] which is clearly illustrated in Figure 2c. A Fickian diffusion process is known to proceed with a concentration gradient into the sample.[12] Such a concentration gradient represents a situation in which the front velocity is more rapid in relation to the diffusivity than it was at room temperature. It can be said that the gradient is necessary to "supply" the advancing front with methanol at a sufficient rate. So, the concentration at the front decreases as penetration proceeds, and this is presumably responsible for the observed decrease in front velocity (Figure 2b).

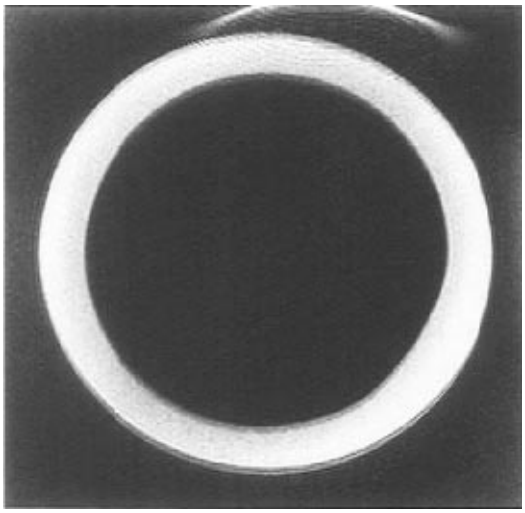

Figure 1. Typical image of the diffusion of MeOH in a PMMA rod at the lowest temperature (26 °C).

As was mentioned earlier, the time dependence of the diffusion process can be expressed using the fitting parameter n out of eq 1. This value n has been calculated at different temperatures, for the diffusion distance s as well as for the distance d, to evaluate the time dependence of the diffusion of methanol in PMMA as a function of temperature (see Figure 3). A 95% confidence interval for calculating n is shown. Here, it is again shown that transport kinetics shift from almost Case II behavior at 26 °C ($n = \pm 1.0$) to almost Case I behavior at 58 °C ($n = \pm 0.5$). Since methanol is a poor

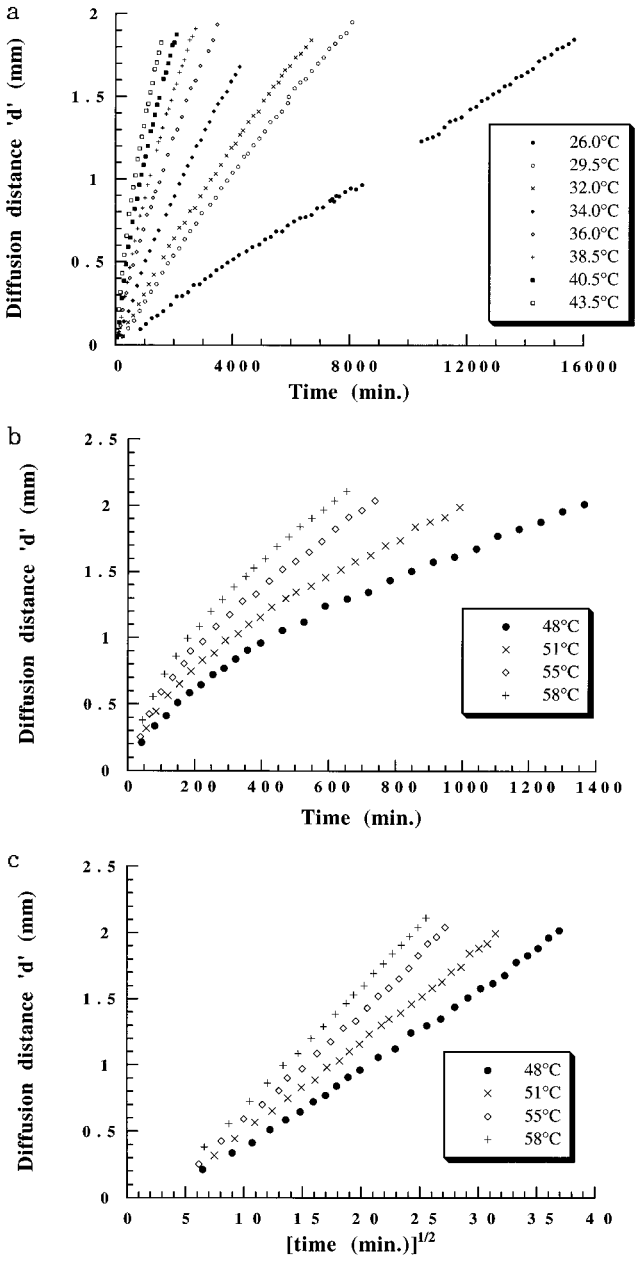

Figure 2. Diffusion distance d of methanol into PMMA for (a) the temperatures 26−43.5 °C as a function of time, (b) the temperatures 48−58 °C as a function of time, and (c) the temperatures 48−58 °C as a function of square root of time.

solvent for PMMA (the solubility parameter, δ, of PMMA is 9.1 and that of methanol is 14.5), the extent of swelling in this case is minor (±15% increase in diameter). Thus, the swelling may not have a major influence on the transport kinetics of methanol in PMMA. It can be noticed that the two curves in Figure 3 are more or less parallel. Thomas and Windle[23] introduced a theory that accounts for the phenomenon of Case II diffusion, which is observed when glassy polymers are swollen in organic penetrants. The mathematical development is in general that it can describe the range of anomalous behavior between the Fickian and Case II extremes. The theory explains the process in terms of two basic parameters: the diffusion coefficient D and the flow viscosity or "creep" of the glassy polymer, η_0. They explored the effect of changes in D and $1/\eta_0$ on the process by calculating penetrant profiles and total sorption plots. Two other characteristic parameters can be derived. They are the induction

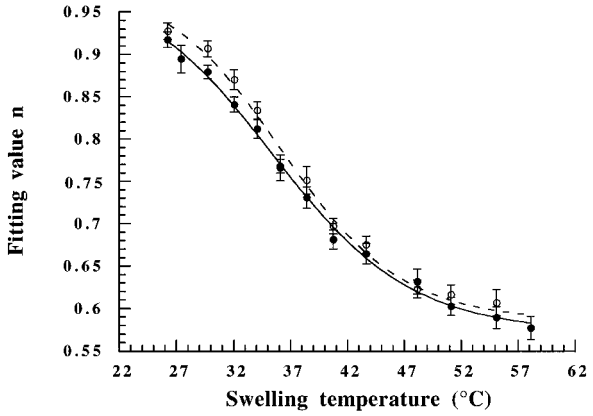

Figure 3. Fitting value n as a function of swelling temperature (°C) for (a) the distance s (●, —) and (b) the distance d (○, – – –). A 95% confidence interval for calculating n is shown.

Table 1. Results of the Fitting of the Sigmoidal Character (Fit 1 is the for the Distance *s* and Fit 2 is for the Distance *d*) in Figure 3[a]

	fit 1	fit 2
n_l	0.98 ± 0.03	0.98 ± 0.04
n_h	0.57 ± 0.02	0.58 ± 0.03

[a] n_l is the value in the lower temperature limit, and n_h is the value in the upper temperature limit.

time, t_{ind}, which is the extrapolation of the linear (or near linear) portion of the sorption curve to the time axis, and the total time taken for the front to traverse from the surface to the central plane, t_{tr}. These two parameters have been plotted as contours on log $1/\eta_0$ versus log D coordinates, which enables them to distinguish certain regions of diffusion types. The constant velocity at which the front traverses the specimen, thus the front traverse time, in the Case II process depends equally on the viscous flow rate ($1/\eta_0$) and on the diffusivity or diffusion coefficient (D). During Fickian diffusion, front traverse rate only depends on D. The rate $1/\eta_0$ has become too large to exert any rate-controlling influence on the transport process. When temperature increases, reduction of the diffusivity in relation to the viscous flow rate takes place, making the viscous flow rate less rate-controlling. This leads to an increase in the concentration gradient behind the fronts and destroys the linearity of the kinetics with time (=Case II), tending toward square root dependence with time (=Fickian).

This gradual change from Case II to Fickian behavior (Figure 3) has a sigmoidal character.[24] We searched for the best fitting S-shaped model curve, and these results are shown in Table 1. As one can see, $n = 1.0$ in the lower temperature limit and approaches almost 0.5 in the higher temperature limit ($n = \pm 0.57$). Pure Fickian diffusion does not take place under these circumstances. The region of inflection (i.e., where the second derivative equals zero) is situated around 35−36 °C. This sigmoidal change as a function of swelling temperature can be related with a change of the glass transition temperature, T_g, of the polymer matrix during the experiments. The sorption of organic solvents increases free volume in a polymer and thus depresses the glass transition temperature. The degree of depression in T_g is dependent on the solubility; the greater the equilibrium solubility of the solvent in the polymer, the lower the effective T_g. On the other hand, the effective glass transition temperature (i.e., of the swollen polymer)

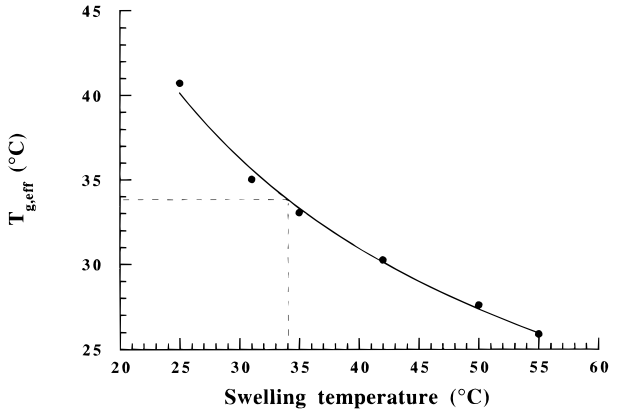

Figure 4. Effective glass transition temperature, $T_{g,eff}$, as a function of swelling temperature (°C).

decreases with increasing temperature of methanol treatment. The glass transition temperature of the original PMMA used in this study is 115 °C. The material is not purely atactic (T_g of atactic PMMA is 104 °C) but contains some amount of syndiotactic sequences (T_g of syndiotactic PMMA is ±130 °C and that of isotactic PMMA is 45 °C). The effective glass transition temperatures, measured as the point of inflection in the DSC-curves and corresponding to the different swelling temperatures, are shown in Figure 4. It can be noticed that when the swelling temperature, i.e., the temperature of the bulk methanol, is below 34 °C, the glass transition temperature of the imbibed PMMA will be above 34 °C and vice versa. This point, i.e., the crossover temperature, corresponds very well with the region of inflection in Figure 3. So, one could say that at this point the glass transition temperature of the imbibed region equals the swelling temperature. At temperatures above this point, the working temperature will be above the effective T_g of the imbibed region and this distinction increases with increasing swelling temperature. It could be said that the imbibed region behaves more and more as a rubbery region, which explains the tendency toward Fickian diffusion as the swelling temperature increases. Beneath this point, the working temperature will be below the effective T_g of the imbibed region. The imbibed region approaches the characteristics of a glassy polymer and Case II diffusion will take place at lower temperatures. To preserve the presence of concentration gradients in the imbibed region during the diffusion process and to avoid the imbibed region reaching full saturation, DSC measurements were performed on partially saturated samples (remaining glassy core).

Figure 5 shows a schematic representation of the phase diagram PMMA−methanol (analogous to the phase diagram PMMA−butanol[25]). Region III is a phase-separated region. The solution, in this concentration range, will separate into a polymer-rich phase and a solvent-rich phase. The line between regions I and II is the $T_g-\varphi_2$ relationship, where φ_2 is the polymer weight fraction. Region II is the glassy region and region I is the rubbery region. As was shown in the previous paragraph, it is known that, when PMMA is swollen at 35−36 °C, the T_g of the material equals almost 35−36 °C. This is situation a in the phase diagram. When PMMA is swollen in methanol below 35−36 °C, less solvent will be taken up by the polymer matrix (shift to the right in Figure 5) and T_g will increase (b′). The polymer matrix remains glassy (situation b). At conditions just beside the T_g line, the

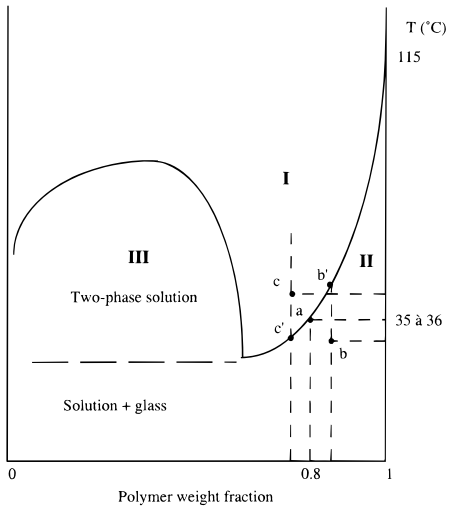

Figure 5. Schematic representation of the phase diagram PMMA−methanol.

mobility of the polymer chain segments will be higher than further away from this line in the glassy region. When swelling temperature decreases, the mobility of the polymer chain segments will decrease due to an increase of T_g of the matrix and one shifts to a situation where diffusion characteristics will tend more toward Case II. It must be mentioned that this shift takes place in a small area underneath the T_g line (situation b is set further from the T_g line for the sake of clarity; normally this point is situated fairly near this line). When PMMA is swollen in methanol above 35−36 °C, the solvent amount will increase (shift to the left in Figure 5) and T_g will decrease (c′). The polymer matrix becomes rubbery (situation c). When swelling temperature increases, the mobility of the matrix will increase due to a decrease in T_g. This mobility increases when going further from the T_g line, thus going to a situation where diffusion kinetics approach Fickian characteristics. This effect is restricted to a small area above the T_g line (also normally situated fairly near the T_g line). Out of weight gain measurements, it is known that the equilibrium solubility (volume fraction) of methanol in PMMA changes from ±0.20 at 30 °C toward ±0.22 at 39 °C.

The change of n with swelling temperature (Figure 3) shows a similar temperature dependence as the mechanical behavior of an ordinary, viscoelastic polymer.[26] We go from a plateau at $n = \pm 1.0$ (=Case II, generally assigned to diffusion in a glassy polymer) to a plateau at $n = \pm 0.5$ (=Fickian, generally assigned to diffusion in a rubbery polymer). The transition takes place around the temperature where the glass transition temperature of the swollen material equals the swelling temperature. For some swelling temperatures, the temperature course of the storage modulus E' has been investigated. Figure 6 shows the change of the value of E' measured from DMA for each swelling temperature at the corresponding temperature, because this value reflects the mechanical behavior during the diffusion experiment. The relative error (%) on E' changes from ±20% at 25 °C to ±5.5% at 60 °C. As can be clearly seen, the change of E' with swelling temperature also has a sigmoidal character. This illustrates that the diffusion kinetics (parameter n) are principally coordinated by the mechanical response of the polymer matrix to the presence of the solvent molecules. Due to the fact that these experiments are performed at a frequency of 1 Hz, the point where the transition from Fickian to

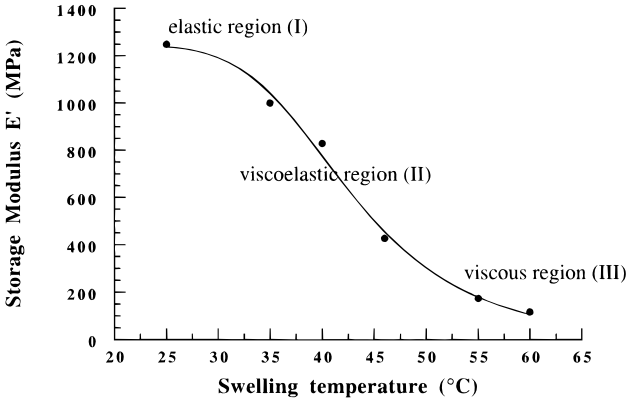

Figure 6. Storage modulus E' as a function of swelling temperature (°C).

Case II diffusion takes place is shifted somewhat to higher temperatures. Imaging and DSC experiments are carried out at a frequency of 0 Hz.

Hopfenberg and Frisch[27] succeeded in describing all observed behavioral features for one specific polymer−penetrant system in a diagram of temperature versus penetrant activity, which seems to be of general significance for amorphous polymers. The region of Case II sorption in their diagram is separated from the Fickian diffusion region by a region where both relaxation and diffusion mechanisms are operative, giving rise to diffusional anomalies. A curve representing the effective glass transition temperature $T_{g,eff}$ of the polymer−penetrant system goes through the center of this region of anomalous diffusion. Outstanding work was done by Vrentas et al.[28] They introduced an important dimensionless quantity which is characteristic for polymer-solvent systems: the diffusional Deborah number, by analogy to the flow Deborah number used to describe the behavior of non-Newtonian fluids. It is defined in the following way:

$$De = \frac{\lambda}{\Theta} = \frac{\text{characteristic relaxation time}}{\text{characteristic diffusion time}} \qquad (3)$$

The characteristic time for penetrant diffusion, Θ, is generally written as

$$\Theta = L^2/D \qquad (4)$$

where L is a characteristic diffusion length, and D is the diffusion coefficient of the penetrant in the polymer. The characteristic relaxation time, λ, may be expressed as a mean relaxation time using

$$\lambda = \frac{\int_0^\infty tG(t)\,dt}{\int_0^\infty G(t)\,dt} \qquad (5)$$

where $G(t)$ is the shear relaxation modulus which appears in linear viscoelasticity theory, and the denominator is the viscosity at zero shear rate. Vrentas et al. attempted to establish regions of Fickian diffusion and non-Fickian transport of the penetrant in the polymer as a function of penetrant concentration and temperature by determining limiting values of the Deborah number. Also they found that Case II diffusion is separated from Fickian diffusion by an anomalous region and central through this region runs the line of $T_{g,eff}$. Above T_g (see region III in Figure 6), viscous diffusion takes place. The imbibed region behaves like a viscous fluid in diffusive transport, and, hence, mass transfer at all penetrant concentrations follows the classical theory of diffusion with a diffusion coefficient which is strongly dependent on concentration. Around the effective T_g (region II in Figure 6), diffusion becomes viscoelastic and at lower temperatures (region I in Figure 6), the system behaves elastically in a diffusion process, and a spectrum of transport behavior can be observed depending on the ultimate penetrant concentration in the sample. For small amounts of penetrant, Fickian diffusion is also observed. At higher penetrant activities, anomalous diffusion and extreme anomalous effects such as Case II transport, solvent crazing, and fracture are observed. This theory again illustrates that the temperature dependence of the diffusion kinetics (Figure 3) can be correlated with a change of the mechanical behavior of the polymer matrix in the presence of the penetrant (Figure 6). At temperatures below the effective T_g of the imbibed material, movement of the polymer segments in response to an osmotic swelling stress at the front is the rate-controlling process. Above $T_{g,eff}$, the matrix behaves like a viscous fluid and diffusion becomes the rate-controlling process.

Table 2. Values for ν (10^{-9} m/s) and D (10^{-11} m^2/s) for Various Temperatures for the Diffusion Distances s and d

	ν (10^{-9} m/s)		D (10^{-11} m^2/s)	
temp (°C)	without correction (s)	with correction (d)	without correction (s)	with correction (d)
26	2.4	2.0		
27.5	2.7	2.4		
29.5	4.3	3.6		
32	5.8	4.9		
38.5			5.8	3.7
40.5			7.2	4.5
43.5			9.3	5.4
48			9.8	6.1
51			13.0	7.9
55			18.6	11.7
58			23.3	13.9

Activation Energies. Case I (Fickian) diffusion is controlled by the diffusion coefficient. In Case II diffusion, the basic parameter is the constant velocity of an advancing front which marks the innermost limit of penetration or dispersal of the penetrant and is the boundary between (stressed equilibrium) swollen gel and the glassy core of the sample.[29] The square of the slope of a linear least-squares fit of a plot of the diffusion distance versus square root of time provides a diffusion coefficient for the swelling temperatures after the point of inflection in Figure 3. For the lower temperatures where the diffusion characteristics approach Case II, i.e., before the point of inflection, ds/dt and dd/dt is the rate at which the front is moving into the glassy core. Table 2 lists the penetration rates ν (10^{-9} m/s) and diffusion coefficients D (10^{-11} m^2/s) for the lower and higher swelling temperatures respectively. As can clearly be seen, correcting for the change in diameter of the polymer matrix, which takes place upon swelling, gives smaller values for ν and D. Figures 7 and 8 show the temperature dependence of the penetration rate and the diffusion distance, respectively (ln ν or ln D versus $1/T$). The plots show a linear relationship, which means that Arrhenius' law is applicable. The values for the activation energy E_A, which can be derived from these plots, are listed in Table 3. Also here, again it is shown that, due to the minor swelling, correction for shape change does not have much influence on the values derived for E_A. The E_A values for Case II diffusion lie in the range of values reported[21−23,30] for creep of glassy

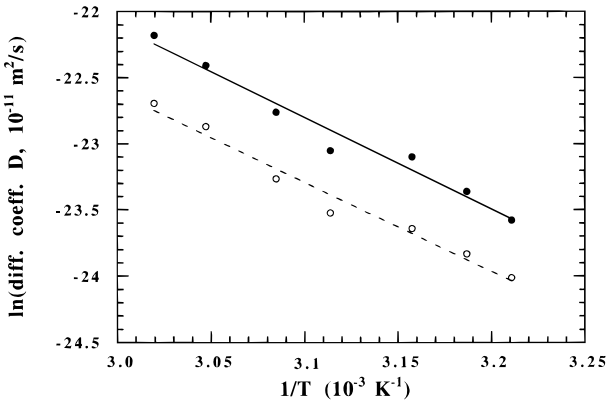

Figure 7. Apparent activation energies for diffusion (=Case I) of methanol in PMMA for the diffusion distances *s* (●, —) and *d* (○,– – –).

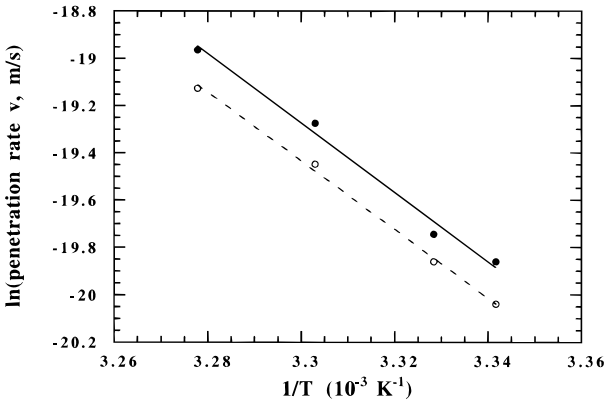

Figure 8. Apparent activation energies for relaxation (=Case II) during methanol absorption in PMMA for the diffusion distances *s* (●, —) and *d* (○,– – –).

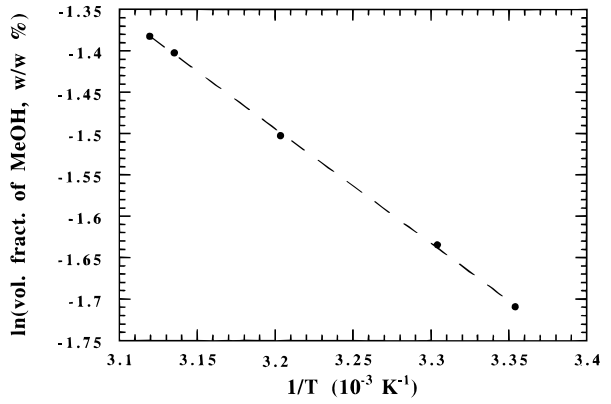

Figure 9. Van't Hoff plot for the temperature dependence of equilibrium solubilities.

Table 3. Activation Energies E_A for Case I and Case II Calculated for the Diffusion Distances *s* and *d*

	E_A in kJ mol^{-1}	
	without correction (*s*)	with correction (*d*)
Case I	57.5 ± 4.5	56.1 ± 4.1
Case II	122.2 ± 9.3	120.9 ± 4.4

PMMA, the rate-controlling factor of Case II, i.e., 25–30 kcal mol^{-1} (=104–125 kJ mol^{-1}). The E_A values for Case I diffusion match the value of 14 kcal mol^{-1} (=60 kJ mol^{-1}) mentioned by Thomas and Windle.[23]

Heat of Mixing. For a few temperatures, equilibrium solubility of methanol in PMMA has been determined by weighing (see Figure 9). The endothermic heat of mixing, ΔH_s°, is 2.76 kcal mol^{-1} (or 11 ± 0.1 kJ mol^{-1}). This agrees very well with the values obtained by Hopfenberg et al.,[31] 2.8 kcal mol^{-1}, and Thomas and Windle,[22] 3 kcal mol^{-1}. It should be noted that very high molecular weight PMMA was used here. Equilibrium solubilities (0.18–0.25 in the chosen temperature range) are therefore slightly lower than obtained by Hopfenberg and Windle.

Conclusion

At ambient temperatures, the absorption of methanol by PMMA follows Case II kinetics. The penetration of the sharp front is linear with time. As the temperature of absorption is increased up to near the boiling point of methanol, departures from Case II kinetics become increasingly significant and the exponent of time, *n*, describing the methanol uptake, approaches the typical value for Fickian diffusion, i.e., 0.5. The main reason for this transition is an increase in viscous flow rate, which is not matched by a corresponding increase in diffusivity. This results in a more prominent concentration gradient behind the front, which in the extreme leads to the re-establishment of Fickian kinetics. This transition from Case II to Fickian diffusion takes place at a temperature around the effective T_g of the system. It is also illustrated that the change of the storage modulus E' with the swelling temperature follows a temperature dependence similar to the parameter *n*. So, one can conclude that the mechanical response of the polymer matrix in response to the presence of the solvent molecules is an important factor controlling the diffusion process.

Acknowledgment. We are grateful to the IWT (Flemish Institute for the Promotion of Scientific Technological Research) for financial support of this research. The authors also thank Prof. Dr. H. Berghmans (K. U. Leuven) for his valuable comments, Prof. Dr. J. Mullens for putting his DMA equipment at our disposal, Drs. T. Roels (K. U. Leuven) for assistance with the DSC measurements, and Mr. J. Kaelen for solving some practical problems.

References and Notes

(1) Chandy, M. C.; Rajasekharan Pillai, V. N. *Polym. Int.* **1995**, *37*, 39.
(2) Sammes, N. M.; Vohora, S. *J. Mater. Sci. Lett.* **1995**, *14*, 483.
(3) Shibusawa, T. *J. Polym. Sci., Part B: Polym. Phys.* **1993**, *31*, 29.
(4) Shailaja, D.; Yaseen, M. *Eur. Polym. J.* **1992**, *28*, 1321.
(5) Ramaraj, B.; Radhakrishnan, G. *J. Appl. Polym. Sci.* **1994**, *51*, 979.
(6) Fritzsche, A. K.; Narayan, R. S. *Chem. Econ. Eng. Rev.* **1987**, *19(205)*, 19.
(7) Nakagawa, T. *Chem. Econ. Eng. Rev.* **1987**, *19(205)*, 32.
(8) Rautenbach, R.; Albrecht, R. *Int. Chem. Eng.* **1983**, *27*, 10.
(9) Frisch, H. L. *Polym. Eng. Sci.* **1980**, *20*, 2.
(10) Vrentas, J. S.; Duda, J. L.; Huang, W. J. *Macromolecules* **1993**, *26*, 1841.
(11) Alfrey, T.; Gurnee, E. F.; Lloyd, W. G. *J. Polym. Sci., Part C: Polym. Lett.* **1966**, *12*, 249.
(12) Webb, A. G.; Hall, L. D. *Polymer* **1991**, *32*, 2926.
(13) Ercken, M.; Adriaensens, P.; Vanderzande, D.; Gelan, J. *Macromolecules* **1995**, *28*, 8541.
(14) Hyde, T. M.; Gladden, L. F.; Mackley, M. R.; Gao, P. *J. Polym. Sci., Part A: Polym. Chem.* **1995**, *33*, 1795.
(15) Ilg, M.; Pfleiderer, B.; Albert, K.; Rapp, W.; Bayer, E. *Macromolecules* **1994**, *27*, 2778.
(16) Perry, K. L.; McDonald, P. J.; Clough, A. S. *Magn. Reson. Imaging* **1994**, *12*, 217.
(17) Perry, K. L.; McDonald, P. J.; Randall, E. W.; Zick, K. *Polymer* **1994**, *35*, 2744.
(18) Cody, G.; Botto, R. E. *Macromolecules* **1994**, *27*, 2607.
(19) Komoroski, R. A. *Anal. Chem.* **1993**, *65*, 1068A.

(20) Grinsted, R. A.; Koenig, J. L. *Macromolecules* **1992**, *25*, 1229.
(21) Thomas, N. L.; Windle, A. H. *Polymer* **1980**, *21*, 613.
(22) Thomas, N. L.; Windle, A. H. *Polymer* **1978**, *19*, 255.
(23) Thomas, N. L.; Windle, A. H. *Polymer* **1982**, *23*, 529.
(24) Crank, J. *The Mathematics of Diffusion*; Clarendon Press: Oxford, 1975; Chapter 11.
(25) Vandeweerdt, P.; Berghmans, H.; Tervoort, Y. *Macromolecules* **1991**, *24*, 3547.
(26) Sperling, L. H. *Introduction to Physical Polymer Science*; John Wiley & Sons, Inc.: New York, 1992; Chapter 8.
(27) Hopfenberg, H. B.; Frisch, H. L. *J. Polym. Sci., Part C: Polym. Lett.* **1969**, *7*, 405.
(28) Vrentas, J. S.; Jarzebski, C. M.; Duda, J. L. *AIChE J.* **1975**, *21*, 894.
(29) Frisch, H. L. *Polym. Eng. Sci.* **1980**, *20*, 2.
(30) Harmon, J. P.; Lee, S.; Li, J. C. M. *Polymer* **1988**, *29*, 1221.
(31) Hopfenberg, H. B.; Nicolais, L.; Drioli, E. *Polymer* **1976**, *17*, 195.

MA960155K